ELSEVIER

Polymer 40 (1999) 4001–4011

polymer

The effect of specific interactions on dye transport in polymers above the glass transition

A.T. Slark[1,*], P.M. Hadgett[2]

ICI Imagedata, Brantham, Manningtree, Essex, C011 1NL, UK

Received 17 December 1997; accepted 18 August 1998

Abstract

The transport of a functionalised dye solute has been studied in various amorphous polymers above the glass transition temperature. An azo dye containing two hydroxyalkyl groups was transferred from a constant dye-donor polymer matrix to a variety of dye-acceptor polymer matrices using dye diffusion thermal transfer printing. Using the solution–diffusion model of permeability as the starting point, equations were developed to correlate solute transport with dye and polymer structural characteristics. Diffusivity is strongly influenced by polymer T_g whereas solubility is controlled by the balance of physical forces and specific interactions between dye and dye-acceptor polymer. An excellent correlation was established for permeability as a function of polymer T_g, dye–polymer solubility parameter difference and dye–polymer specific interaction as characterised by the infrared shift of solute O–H vibration. This predicted that maximum permeability would be obtained via a combination of low T_g, matched dye–polymer solubility parameters and strong specific acid–base dye–polymer interactions.

Keywords: Transport; Permeability; Dye

1. Introduction

In previous studies on the permeability and diffusion of solutes in polymer matrices, distinctions have been made between small molecules (gases) and large molecules (liquids and vapours) which interact strongly with the polymer [1]. For diffusivity, it is generally accepted that for translational motion of a solute to occur, there must be a space of sufficient size for the molecule to move into. It was established that diffusivity partly depends on the size of the solute and that it is possible that diffusion rates can be coupled to relaxational processes in polymers [2]. Molecules comparable with, or larger in size than the polymer repeating unit require a co-operative movement of several polymer segments to take place. Such molecules will require the large space created by the chain co-operative movements characteristic of T_g [3] and are known to exhibit a step change in the diffusion coefficient at T_g. There are many cases where the solute diffusion coefficients have been expressed by molecular models in an Arrhenius form with an associated activation energy [4–10]. In contrast, several authors have illustrated that the temperature dependence of the diffusion coefficient is adequately described using a free volume interpretation [11–18].

The control of dye transport is an important phenomenon in the dyeing of polymer fibres for coloured fabrics and the dyeing of polymer films for imaging applications. There are several publications in the literature where the importance of the polymer glass transition temperature to dye transport is highlighted in the conventional dyeing of fibres [19,20] and films [21–23]. A variety of publications have illustrated that the variation of dye diffusion coefficient above T_g is well represented by the Williams-Landel-Ferry (WLF) equation [24]. Generally, this was proved at low dye concentrations [25–27] but it is also applicable at high concentrations provided plasticisation is taken into account [28]. The control of dye delivery is also important in dye diffusion thermal transfer printing, which is a method for producing high quality continuous tone colour images from an electronic source [29]. The printing process involves the transfer of dye from a donor ribbon to an acceptor sheet which are brought in close contact at high temperature and pressure. The temperature of dye transfer and print time can vary but maximum values are typically 300°C and 12 ms, respectively. In addition to being technologically

* Corresponding author. Tel.: +1642-432405; fax: +1642-437768.

[1] Current address: ICI Acrylics, P.O. Box 90, Wilton, Middlesbrough, Cleveland, TS90 8JE, UK. Tel.: 01642 454144; fax: 01642 437768.

[2] Current address: 140 Coalpit Hill, Talke, Stoke-on-Trent, Staffs, ST7 1PN, UK.

0032-3861/99/$ - see front matter
PII: S0032-3861(98)00639-9

important, a thermal transfer printer represents a well-controlled and defined experimental test-bed for studying the diffusion of dyes in polymers. Typically, both the donor ribbon and acceptor sheet for thermal transfer printing are multilayered structures, with each layer performing a particular function [29]. The dye transfers from a polymer coating in the donor sheet (dye-donor) to an acceptor polymer coating in the receiver sheet (dye-acceptor). It was shown that the mechanism for dye transfer is diffusion between polymers rather than sublimation [30]. Therefore, the dye transfer process can be viewed as permeability from a dye-donor polymer to a dye-acceptor polymer where the temperature of transport is above the glass transition temperatures of both the donor and acceptor matrices. The dye transfer process was modelled previously. Hann and Beck [29] illustrated that the use of a model involving diffusion coefficients and partition coefficients was reasonable in predicting dye transfer. More recently, Shinozaki and Hirano [31] have proposed a mechanism involving adsorption followed by diffusion.

Recently, we have published a number of articles related to the transport of dyes in polymers. Initial work was focussed on the release of dye from a variety of dye-donor matrices to a constant dye-acceptor, where it was demonstrated (at constant dye concentration) that the transport of the dye molecules was controlled by the T_g of the dye–polymer mixture in the donor film [28]. This relationship was extensive for all types of chromophore and polymer studied. The data was found to fit well with free volume considerations and the WLF equation by using the T_g of the dye–polymer blend in the donor matrix. The effects of intermolecular forces on the dye–polymer blend T_g's were investigated in detail, as the T_g of the dye–polymer blend was critical [32,33]. Depending on the dye–polymer combination, the dye was found to decrease the T_g of most polymers (plasticisation) while increasing the T_g of others (antiplasticisation). The dye–polymer blend T_g was found to depend on the polymer T_g, the dye solute T_g, their relative concentrations and dye–polymer affinity. Increasing dye–polymer affinity produced stronger interaction between dye and polymer leading to higher T_g of the dye–polymer blend. Excellent correlations were established between T_g enhancement and dye–polymer solubility parameter match. Solubility parameters indicated that the combination of polar and hydrogen bonding forces controlled the elevation of T_g, as the best correlation was obtained by neglecting the dispersion forces. Subsequently [34], it was demonstrated that the Kwei equation could be applied to explain the effects of intermolecular forces on the dye–polymer blend T_g's as the Kwei q parameter correlated well with enhanced dye–polymer affinity. More recently, we have published studies on dye transport to the dye-acceptor. Rutherford backscattering was used to study dye diffusion into various polymer films with different T_g using a sulphur atom in the dye as a label [35]. Both the diffusion coefficients and the depth of penetration of the dye were found to be controlled by the T_g of the dye-acceptor polymer matrix. For this study, the dye/polymer interactions were similar and the diffusion coefficients were found to be in good agreement with free volume theories of diffusion. When the affinity between dye and dye-acceptor varies, we have also demonstrated that dye transport to a dye-acceptor is a function of both diffusivity and solubility [36]. An excellent correlation was made for dye transport as a function of dye-acceptor polymer T_g and the solubility parameter difference between dye and dye-acceptor polymer. The limit of applicability of this previous work was defined as the transport of large solutes in amorphous polymers above T_g and in the absence of strong specific interactions.

We have also recently published our studies on dye–polymer systems where strong specific acid–base interactions are present. The interactions of hydroxyl-functionalised dye solute molecules were investigated in polymers with a wide variety of electron-donating functional groups using infrared spectroscopy [37,38]. There are two main species present which occur in all systems, the dye–polymer intermolecular interaction between the dye hydroxyl group and the polymer electron-donating functional group (D–P) and the dye–dye self-association interaction between dye hydroxyl groups (D–D). The strength of the D–P interaction is independent of dye concentration, the number of hydroxyl groups and the flexibility of the dye molecule but has a pronounced dependence on the polymer environment with the D–P strength increasing systematically with the electron-donating power of the polymer. The strength of the D–D interaction is independent of the flexibility of the dye molecule but is dependent on the dye concentration, the number of hydroxyl groups and the polymer environment (relatively weak dependence for the latter). The D–D interactions are usually stronger in nature than D–P interactions except for amide and amine environments. The relative amounts of D–P and D–D interactions are related to the relative strengths of D–D/D–P and depend on dye concentration, the number of dye hydroxyl groups and the composition of the polymer environment. For systems capable of specific acid–base dye–polymer interactions we recently proposed a model for the transport of a fixed dye solute from a common dye-donor using the solution–diffusion model of permeability as a starting point [39]. Equations were developed to correlate solute permeability with dye and dye-acceptor polymer structural characteristics. In this analysis, it was assumed that diffusivity at high temperature was a function of free volume and polymer T_g whereas solubility was controlled by the balance of endothermic physical forces and exothermic specific interactions between dye and dye-acceptor polymer. The model predicts that high permeability will be obtained when the dye-acceptor T_g is low, the solubility parameters of dye and dye-acceptor polymer equal and specific interaction between dye and dye-acceptor polymer strong. The purpose of this article is to compare the experimental data against this model. The influence of structural parameters on the

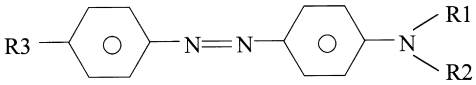

R1 = -CH_2-CH_2-CH_2-OH
R2 = -CH_2-CH_3
R3 = -CH_2-CH_2-OH

Fig. 1. Structure of the dye solute containing two peripheral hydroxyalkyl groups.

transport of a dye solute containing hydroxyl groups is investigated, from a fixed dye-donor to a number of different dye-acceptor polymers with a variety of chemical compositions (with differences in T_g, solubility parameter and electron-donating functional group character).

2. Method

2.1. Materials

Fig. 1 shows the structure of the dye solute used in this study, which was supplied by Zeneca Specialties. The dye contains a central stiff aromatic core to which are attached two alkyl chains with terminal hydroxyl groups. These hydroxyl groups have the potential to provide specific interactions between the solute and polymers with electron-donating functional groups. The functionality directly attached to the central aromatic core was minimised so that there are no additional functional groups positioned directly on the phenyl rings. This simplification allows infrared spectroscopy to be used to characterise dye interactions involving hydroxyl groups. Different polymer structures were used as matrices for the solutes, containing a wide variety of electron-donating functional groups (phenyl, chloro, cyano, carboxyl, amide and amine) and these are shown in Table 1 with abbreviations. All polymers were used as supplied.

2.2. Dye–polymer blend donor films

The dye was mixed with poly(vinyl butyral) (PVB) (1 : 1 w/w) and dissolved in tetrahydrofuran (THF) solvent (total solid content = 4.2%(w/w)). Donor films were created by coating this dye–polymer mixture using a wire bar onto a thin 6 μm poly(ethylene terephthalate) (PET) base film, followed by post-heating at 110°C for 20 s to produce a solid coating of a thickness of approximately 1 μm. This treatment has previously been shown to be effective in removing THF to low levels without causing the dye to phase separate [28]. The dye–polymer layer was coated with a thin 0.14 μm layer of poly(styrene-co-butadiene) from a hexane solution. This layer was required to prevent adhesion between the dyecoat and receiver layers under elevated temperature and pressure during the thermal transfer printing process.

2.3. Dye-acceptor films

Acceptor sheets were created by coating 4 μm layers of the dye-acceptor polymers onto PET base (''Melinex 990''

Table 1
Summary of the polymers used as dye-acceptor coatings

Polymer structure	Supplier	Polymer	Functional group	T_g(°C)[a]	$(\delta_d - \delta_p)^2$ (J cm^{-3})[b]	ν_{inter} (cm^{-1})[c]
poly(vinyl chloride)	Polysciences	PVC	–Cl	88.0	4.33	3602
Polystyrene	BDH chemicals	PS	–phenyl	111.0	9.49	3583
poly(iso-butyl methacrylate)	''Neocryl B-700'';Zeneca Resins	PBMA	–COO–	71.5	34.34	3544
Polyester[d]	''Vylon 103'';Toyobo	PE1	–COO–	47.0	0.01	3547
Polyester[e]	''Vylon 200'';Toyobo	PE2	–COO–	69.0	0.00	3547
poly(methyl methacrylate)	''NeocrylB-728'';Zeneca Resins	PMMA	–COO–	122.0	19.18	3541
poly(ethyl methacrylate)	Aldrich Chemical Company	PEMA	–COO–	80.0	22.85	3541
poly(methyl acrylate)	Aldrich Chemical Company	PMA	–COO–	19.5	9.49	3541
poly(vinyl acetate)	BDH Chemicals	PVAc	–COO–	42.0	9.49	3520
poly(styrene-co-acrylonitrile) 75:25 (w:w)	Aldrich Chemical Company	P(S-co-AN)	–CN, –phenyl	110.0	3.53	3518
poly(vinyl pyrrolidone-co-vinyl acetate) 60:40 (w:w)	''VA64'';BASF	P(Vpy-co-Vac)	–CON–, –COO–	62.0	0.40	3368
poly(styrene-co-vinyl-pyridine) 20:80 (w:w)	Aldrich Chemical Company	P(VP-co-S)	–N = ,phenyl	97.0	0.77	3281
poly(vinyl pyridine)	Polysciences	PVP	–N =	90.0	0.00	3279

[a] T_g on film coatings measured by DSC.
[b] Solubility parameter difference calculated by the Fedors method [40].
[c] ν_{inter} is the frequency of infrared absorption resulting from intermolecular bonding between hydroxyl groups and polymer electron-donating functional groups.
[d] Polyester copolymer containing 25% terephthalic acid, 20% isophthalic acid, 5% sebacic acid, 25% neopentyl glycol and 25% ethylene glycol.
[e] Polyester copolymer containing 25% terephthalic acid, 25% isophthalic acid, 25% neopentyl glycol and 25% ethylene glycol.

obtained from *ICI Films*) with a thickness of 125 μm. The polymers were dissolved in solvent and coated onto the PET base using a wire bar. The coatings were dried by placing the receiver sheet in an oven at 140°C for 1 min. THF was used as the solvent for majority of materials with the exception of PMA (toluene) and P(VP-co-VAc) (water).

2.4. Permeability method and evaluation

The donor sheet and receiver sheet were then placed with the dye-donor and dye-acceptor layers in close contact. The transport of dye was initiated by a thermal transfer printer using a head voltage of 12 V and a print time of 12.6 ms. After printing, the donor sheet and receiver sheet were separated and the amount of dye which had transferred to the acceptor layers was determined using a Macbeth TR1224 optical densitometer. These optical density (OD) measurements established the average amount of colour which had diffused into the dye-acceptor and depends on the dye concentration. An average of five measurements was made.

2.5. Differential Scanning Calorimetry

A Perkin–Elmer DSC-4 instrument was used to characterise the glass transitions of the polymers used as dye-acceptor layers. An Indium standard was used for calibration and a heating rate of 20°C per minute was employed. The method used reflected exactly how the polymer coatings were prepared in the permeability investigations. A 4 μm polymer layer was coated onto a 3.5 μm PET substrate using the same method outlined earlier. An identical area of PET substrate without coating, which received the same thermal treatment, was used as a reference. The software subtracted the reference from the sample providing the T_g of polymer coating.

2.6. Solubility parameter determination

Solubility parameters (δ) were calculated according to the group contribution method of Fedors [40] by choosing the appropriate average repeating unit of the polymer structures;

$$\delta = \left(\frac{E}{V}\right)^{1/2}, \tag{1}$$

where E is the sum of the cohesive energy of the functional groups per average repeating unit and V the sum of the molar volume of the functional groups per average repeating unit. The calculations were based on the tabulated group contributions reproduced by van Krevelen [41].

2.7. Infrared spectroscopy

Dye–polymer infrared spectra were obtained by depositing films on to NaCl plates as described elsewhere [37,38] using a Perkin–Elmer 1720X FTIR at a resolution of 2 cm^{-1}. The polymer spectra were digitally subtracted from the dye–polymer spectra producing characterisation of the dye in the polymeric environment.

3. Results and discussion

3.1. Expansion of the solution–diffusion equation

The dye transfer process occurs at temperatures of 150°C–300°C at the interface of dye-donor and dye-acceptor layers, well above the glass transition temperatures of these matrices. It should be noted that the temperature is not discrete during dye diffusion thermal transfer printing. During a particular print time, there is a temperature distribution as the temperature rises, peaks at a maximum and then falls [29]. Therefore, the printing process provides a very well-defined, constant temperature profile or cycle rather than a fixed, single temperature. Previous mathematical modelling [29] indicates that the maximum temperature at the interface between the dye-donor and dye-acceptor polymer matrices is 300°C for a print time of 13 ms. From the solution–diffusion model of permeability [42], the permeability coefficient (P) of a solute in a polymer is given by,

$$P = D{\cdot}S, \tag{2}$$

where D is the diffusion coefficient of the solute in the polymer and S the solubility coefficient. In a related publication [39] we have developed a solution–diffusion model to correlate solute permeability with dye and dye-acceptor structural characteristics. For application to our system, where there is a controlled, specific temperature profile rather than a constant single temperature, P, D, and S are effective coefficients averaged over a constant temperature range. The model was developed to focus on the factors which affect dye transport in the dye-acceptor layer when both the dye solute and the dye-donor are constant. By relating diffusivity to free volume (dependent on T_g), and solubility to the enthalpy of solution (dependent on solubility parameter differences), the effective permeability is given by

$$\ln P = a_3 + b_3\left(\frac{1}{T_g}\right) - c_3(\delta_d - \delta_p)^2, \tag{3}$$

which ignores specific interactions. The equation

$$\ln P = a_4 + b_4\left(\frac{1}{T_g}\right) - c_4(\delta_d - \delta_p)^2 - d_4(\nu_{inter} - \nu_{free}), \tag{4}$$

can be developed by including the effects of specific interactions in the enthalpy term. The transport of the hydroxyalkyl functionalised dye solute was tested according to Eqs. (3) and (4), which exclude and include the effect of specific interactions, respectively, where P is the effective permeability over the temperature cycle as measured by the OD of dye in the dye-acceptor polymer after transfer; OD is a measure of the amount of colour which has diffused into

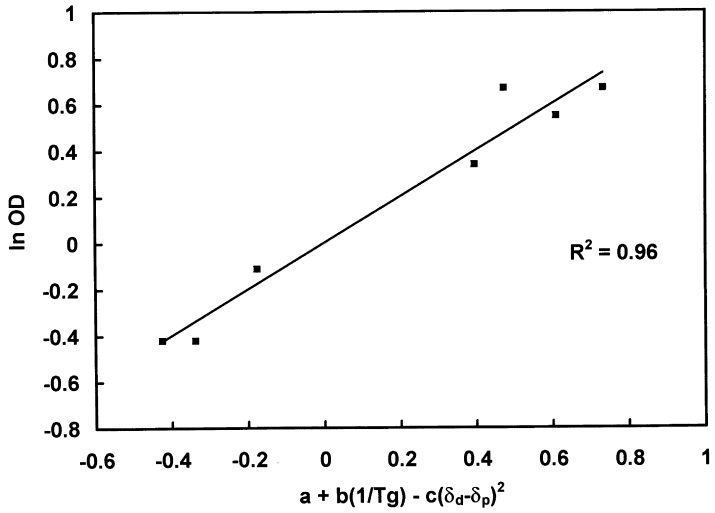

Fig. 2. Dye transport as a function of polymer T_g and dye–polymer solubility parameter difference for dye-acceptor polymers containing ester groups (see Eq. (5)).

the dye-acceptor and is a function of the dye concentration; T_g is the measured glass transition of the dye-acceptor polymer; ($\delta_d - \delta_p$) is the solubility parameter difference between the dye and acceptor polymer calculated using the Fedors method; ($\nu_{inter} - \nu_{free}$) is the difference in frequency of absorption between intermolecularly bonded hydroxyl (ν_{inter}) and free hydroxyl (ν_{free}), as determined by IR spectroscopy; the coefficients in the equations are constants for a particular dye transported to a given set of dye-acceptor polymers at a fixed print-time and constant temperature cycle.

3.2. Constant specific dye–polymer interactions

The functional group types, glass transition temperatures and solubility parameters for all polymers are shown in Table 1. The infrared absorptions resulting from intermolecular interactions between dye hydroxyl group and polymer electron donating functional groups are also illustrated therein. At a fixed concentration, the order of decreasing infrared absorption frequency is –Cl > $-\pi$ > –COO– > –CN > – CON= > –N=. This corresponds to acid–base interaction between dye and polymer becoming stronger as the strength of electron donor in the polymer increases along the series –Cl < $-\pi$ < –COO– < –CN < –CON= < –N=. This is described in more detail elsewhere [37,38]. The polymers were chosen to represent a wide range of acceptor T_g (19.5°C–122°C), dye–polymer solubility parameter difference (0–34 (J cm^{-3})$^{1/2}$) and dye–polymer specific interaction (ν 3602–3279 cm^{-1}).

Fig. 2 shows the regression of permeability as a function

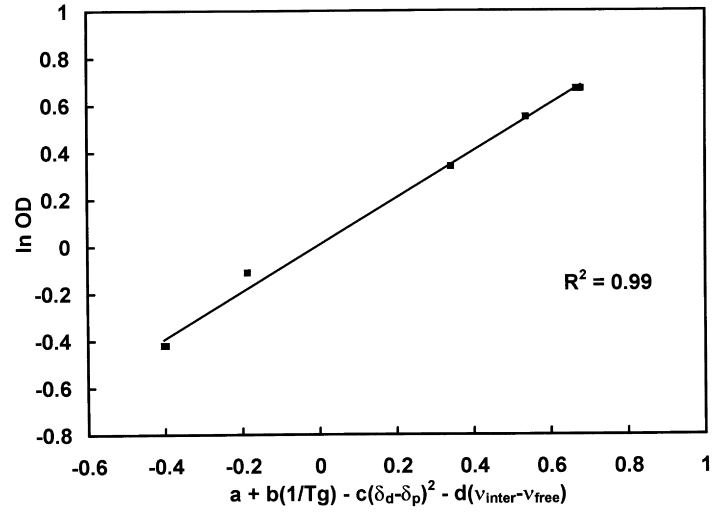

Fig. 3. Dye transport as a function of polymer T_g, dye–polymer solubility parameter difference and specific interactions for dye-acceptor polymers containing ester groups (see Eq. (6)).

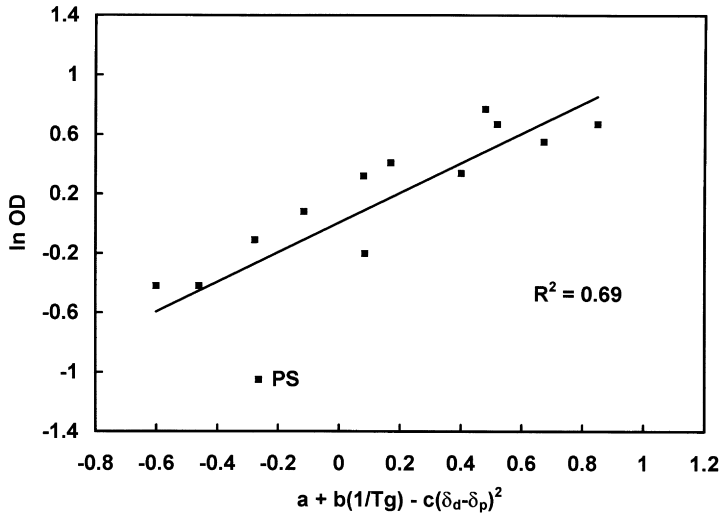

Fig. 4. Dye transport as a function of polymer T_g and dye–polymer solubility parameter difference for all dye-acceptor polymers (see Eq. (7)).

of the combination of T_g and $(\delta_d - \delta_p)^2$, according to Eq. (3), for only those polymers for which the specifically interacting functional group is the same in all cases, i.e., ester carbonyl in polyesters, polymethacrylates and polyacrylates. The correlation is very good producing a regression equation of

$$\ln OD = -2.76 + 1079\left(\frac{1}{T_g}\right) - 0.0207(\delta_d - \delta_p)^2, \qquad (5)$$

and a correlation coefficient of 0.96. This shows that T_g and solubility parameter differences describe the transport well when the polymer electron-donating functional group is constant. For this limited set of data, the hydroxyl absorptions appear in a narrow range (3520–3547 cm^{-1}, see Table 1) as the specific interaction is always between dye hydroxyl and polymer ester carbonyl oxygen. Therefore, dye–polymer specific interactions are very similar in strength and the relative differences small. Fig. 3 shows the same data points but attempts to include the effects of specific interactions according to Eq. (4). The regression equation is given by

$$\ln OD = -3.38 + 972\left(\frac{1}{T_g}\right) - 0.0220(\delta_d - \delta_p)^2 - 0.0106(\nu_{inter} - \nu_{free}), \qquad (6)$$

showing an improved correlation coefficient of 0.99. Despite the similarity of specific dye–polymer interactions in this series they still contribute significantly to the dye permeability. The inclusion of specific interaction serves to improve the correlation which is excellent considering the errors in the different variables. It is expected that OD measurements and T_g measurements individually contribute at least 2% error. Painter and Coleman [43] suggest that at best, solubility parameters are accurate to a level of $\pm 0.8(J\,cm^{-3})^{1/2}$ (i.e. solubility parameter differences subject to errors of 5%). The error resulting from infrared measurements is expected to be small.

3.3. Varying specific dye–polymer interaction

The transport of dye in all polymers related to T_g and dye–polymer solubility parameter differences only is shown in Fig. 4. The regression equation for this relationship is

$$\ln OD = -3.60 + 1368\left(\frac{1}{T_g}\right) - 0.0242(\delta_d - \delta_p)^2, \qquad (7)$$

resulting in scattered data and a relatively inferior correlation coefficient of 0.69. The results suggest that this description of permeability is insufficient for this dye solute in these polymer matrices. This is in contrast with the situation described earlier when the polymer electron donor is kept a constant. Our previous work on a different dye solute also illustrated that such a correlation produced an excellent fit of the data [36] in the absence of specific interactions.Despite the inferior correlation according to Eq. (7), the sign of the coefficients for the T_g and solubility parameter terms remain the same as previous fits, indicating that transport increases when the dye-acceptor polymer T_g is low and/or when the dye–polymer affinity is enhanced. This suggests that T_g and solubility parameters remain important factors but, on their own, are inadequate to define the transport effectively.

Comparing the data in Figs. 2 and 4 suggests that changing the type of electron donor functional group in the polymer causes the relationship to breakdown as a likely result of different specific interactions. Dye transport was then related to T_g, solubility parameter and specific interaction according to Eq. (4) for all polymers. The regression of permeability as a function of these variables resulted in

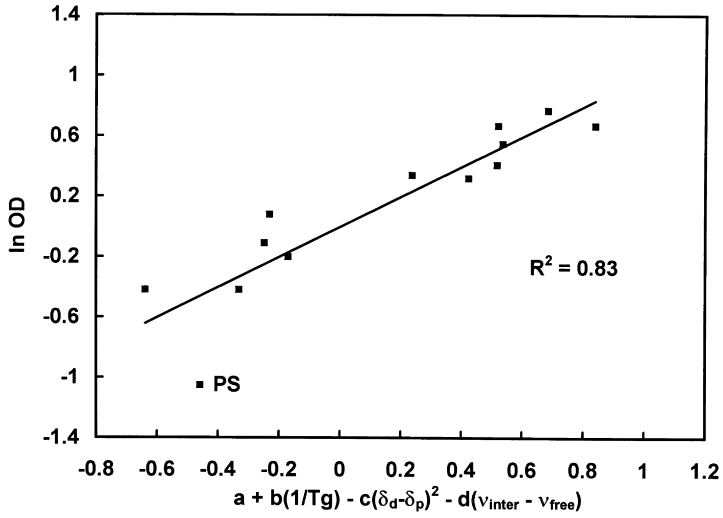

Fig. 5. Dye transport as a function of polymer T_g, dye–polymer solubility parameter difference and specific interactions for all dye-acceptor polymers (see Eq. (8)).

the equation

$$\ln\mathrm{OD} = -4.29 + 1492\left(\frac{1}{T_g}\right) - 0.0158(\delta_d - \delta_p)^2 - 0.0198(\nu_{inter} - \nu_{free}). \quad (8)$$

The data are shown in Fig. 5, producing a correlation coefficient of 0.83. The inclusion of the specific interaction has increased the accuracy of correlation. If the data for polystyrene is omitted, the correlation improves further ($r^2 = 0.93$, see Fig. 6) resulting from the equation

$$\ln\mathrm{OD} = -3.21 + 1178\left(\frac{1}{T_g}\right) - 0.0188(\delta_d - \delta_p)^2 - 0.0128(\nu_{inter} - \nu_{free}). \quad (9)$$

It is important to note that, as ($\nu_{inter} - \nu_{free}$) is negative, the term on the right hand side predicts that increasing the strength of specific interaction between the dye and dye-acceptor polymer leads to *enhanced* dye transport. Although the correlation is significantly improved by the inclusion of specific interactions, there still remains room for improvement. It is necessary to consider the method used to assess the strength of the specific dye–polymer interaction. Fig. 7 shows a schematic illustration of the specific interaction between a dye hydroxyl group and a polymer electron-donating functional group. Hydrogen bonding between these groups affect the bond energies of the polymer–X bond, the H–X bond and O–H bond. In the previous analysis, the frequency of O–H absorption was used as a measure of the total energy of interaction. It should be recognised that ($\nu_{inter} - \nu_{free}$) actually indicates the energy changes to

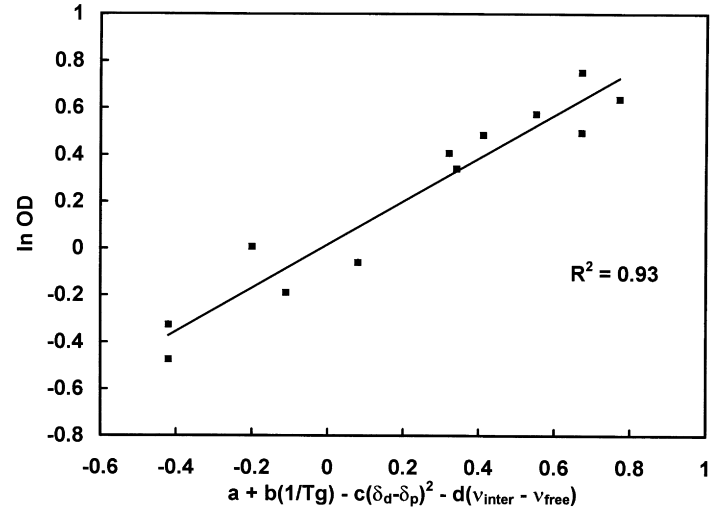

Fig. 6. Dye-transport as a function of polymer T_g, dye–polymer solubility parameter difference and specific interactions for all dye-acceptor polymers, excluding polystyrene (see Eq. (9)).

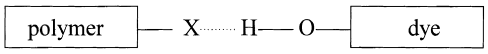

Fig. 7. Schematic representation of the specific interaction between dye solute hydroxyl group and a dye-acceptor polymer with an electron-donating functional group.

the O–H bond only. By using the hydroxyl frequency as a measure of the total energy of interaction it was implicitly assumed that the strengths of polymer–X and H–X are independent of the polymer type and the nature of X. When X is constant, this is a valid assumption, the hydroxyl frequency can be used as an accurate prediction of the overall energy of hydrogen bond formation. This explains why Fig. 3 produces such a good correlation. However, when X varies substantially then this assumption breaks down resulting in the increased scatter, that can be seen in Fig. 5. There have been a number of studies on hydrogen bonding between small molecules which support this. Various experiments have attempted to correlate interaction energies from calorimetric measurements with frequency shifts via infrared spectroscopy. These are explained in detail in the excellent reviews by Murthy and Rao [44] and Pimentel and McClellan [45]. Successful linear correlations were achieved for particular electron acceptors when the electron donors were similar resulting in similar hydrogen bond energies or hydrogen bond lengths. However, studies on phenols and alcohols with a variety of electron donors show that the relationship between the total energy of hydrogen bond formation and hydroxyl frequency shift to be non-linear, especially for electron donors giving rise to exceptionally weak or strong hydrogen bonds (i.e. exceptionally long or short hydrogen bond distances, respectively). This literature suggests that the relationship is better represented by a quadratic function of frequency rather than a linear relationship. Using a quadratic function of the hydroxyl frequency shift, the regression of permeability as a function of the variables produces

$$\ln OD = -4.08 + 1243\left(\frac{1}{T_g}\right) - 0.0192(\delta_d - \delta_p)^2 - 0.00106(\nu_{inter} - \nu_{free}) - 0.000022(\nu_{inter} - \nu_{free})^2. \quad (10)$$

This data is shown in Fig. 8 for all polymers and the correlation coefficient is further increased to 0.90 (from 0.83). This correlation is actually enhanced further if the data for polystyrene is ignored, as shown in Fig. 9. The relationship between permeability and the various parameters is given by

$$\ln OD = -3.20 + 1043\left(\frac{1}{T_g}\right) - 0.0208(\delta_d - \delta_p)^2 - 0.00751(\nu_{inter} - \nu_{free}) - 0.000016(\nu_{inter} - \nu_{free})^2, \quad (11)$$

producing a correlation coefficient of 0.99. This indicates that the interaction with polystyrene is unusually weak (π-electron donor) and might result from the combination of weak electron density which is delocalised rather than specific. Considering the errors previously alluded to, these correlations are excellent.

3.4. Comments on the model

The data demonstrates that T_g, solubility parameters and specific interactions can be used to accurately describe dye transport into a wide variety of dye-acceptor polymers. The dye-donor polymer will also have a significant influence on dye transport, as previously highlighted, but as both the dye and the dye-donor polymer are fixed, the dye-donor system is constant and will not provide any relative change to dye transport in the systems studied. As described in the

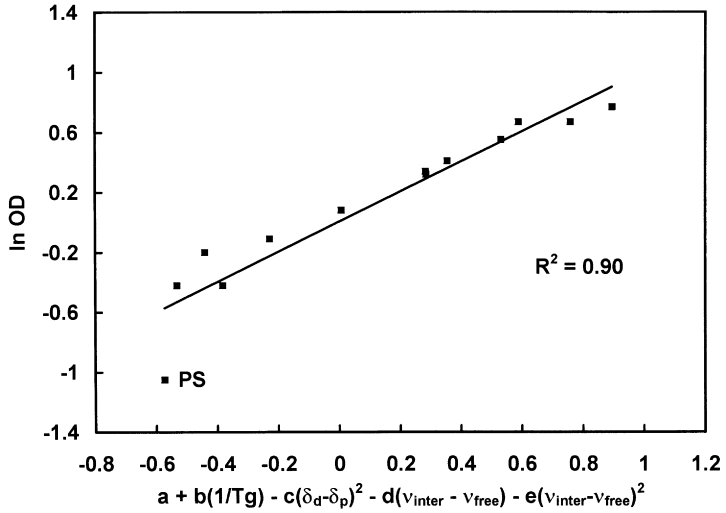

Fig. 8. Dye transport as a function of polymer T_g, dye–polymer solubility parameter difference and specific interactions for all dye-acceptor polymers, where the specific interaction is incorporated via a quadratic function (see Eq. (10)).

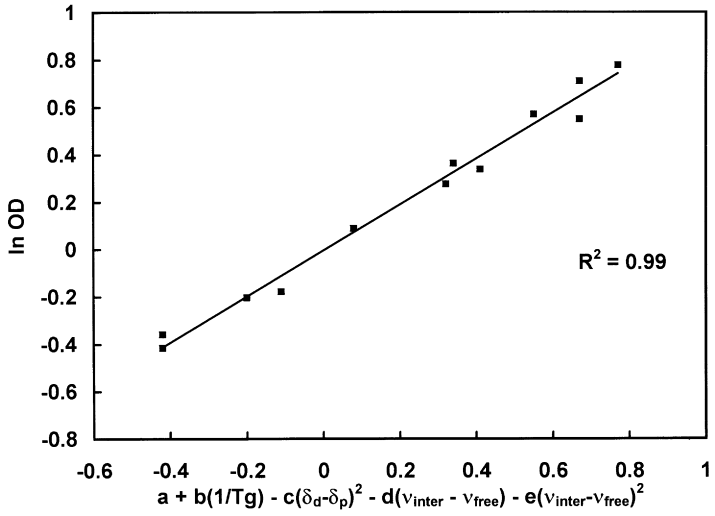

Fig. 9. Dye transport as a function of polymer T_g, dye–polymer solubility parameter difference and specific interactions for all dye-acceptor polymer, except polystyrene, where the specific interaction is incorporated via a quadratic function (see Eq. (11)).

experimental section, the high temperature and pressure experienced in the transport process mean that these are excellent conditions for forming an adhesive joint between dye-donor and dye-acceptor. Something has to be done to enable release at the interface after printing and the very thin styrene-butadiene layer serves this purpose and prevents adhesion. In a similar argument to the dye-donor polymer, as the dye is fixed, any interaction with the release layer will be constant and it can be assumed that this will not vary the amount of dye transport from one system to the next. Both the release layer and the dye-donor polymer will have an absolute effect on dye transport but as the dye is fixed, it is safe to assume that their relative influence is constant and will not vary in the experiments that were conducted.

The development of the solute–polymer solubility terms in Eq. (4) was partly based on analogous work in the field of polymer–polymer blends. In the last decade, Coleman and Painter [43] have pioneered an approach to predict the miscibility of polymer–polymer blends. This approach has been successful in predicting the phase behaviour of a number of polymer–polymer blends involving strong, specific acid–base interactions. This guide to miscibility is based on the assertion that the free energy of mixing of two polymers A and B can be written as:

$$\frac{\Delta G_m}{RT} = \frac{\phi_A}{M_A}\ln\phi_A + \frac{\phi_B}{M_B}\ln\phi_B + \phi_A\phi_B\chi + \frac{\Delta G_H}{RT} \qquad (12)$$

where ΔG_m is the overall free energy of mixing, ϕ_A, ϕ_B the volume fractions of components A and B, M_A, M_B the molecular weights of components A and B, χ the polymer–polymer interaction parameter and ΔG_H the free energy of mixing resulting from specific interactions.

This equation applies to blends where one component is capable of self-association while the other is not, but is capable of intermolecular interaction. The first two terms on the right hand side arise from the combinatorial entropy of mixing. The segmental interaction parameter χ is assumed to represent only physical forces and produces an endothermic contribution to the free energy of mixing. ΔG_H reflects the free energy changes corresponding to specific interactions and produces exothermic contributions to the free energy of mixing. Additionally, χ can be related to solubility parameter differences between the two components whereas ΔG_H can be obtained from equilibrium constants that describe the distribution of hydrogen bonded species present at a particular concentration and temperature. Practically, the miscibility of a polymer–polymer blend is governed by balancing the contribution of the third and fourth terms on the right hand side of Eq. (12). Physical interactions resulting from solubility parameter differences produce unfavourable positive contributions to mixing. This is counteracted by the favourable specific interactions which produce negative contributions to mixing. The degree of interaction depends on the relative magnitudes of these two contributions. These considerations were developed to include the balance of physical forces and specific interactions in our model of dye solute transport (see Eq. (4)). The physical interactions which produce endothermic contributions to the heat of mixing are given by the solubility parameter differences between dye and dye-acceptor polymer. The specific interactions which give rise to exothermic contributions to the heat of mixing are given by the change in frequency of the O–H vibration. The successful use of Eq. (4) illustrates that, provided T_g is constant, dye transport is governed by the relative contribution of physical interactions and specific interactions. The expression dictates that maximum permeability is obtained when the solubility parameters of dye and polymer are identical and when the specific interaction between dye and polymer is strongest. The former provides minimum (i.e. zero) endothermic contribution to mixing whereas the latter

provides a maximum exothermic contribution. Conversely, Eq. (4) predicts that minimum permeability (i.e. barrier effects) is obtained when there are no solute–polymer specific interactions and when the solubility parameter difference between dye and polymer is large. The equation also has the advantage that it is relatively simple to apply compared to other analytical equations in the literature. Application of the equation requires only the measurements of polymer T_g and infrared spectroscopy in addition to solubility parameter calculations; these are all readily accessible.

The results agree with the derived analytical model, part of which assumes that diffusivity is controlled solely by the T_g of the acceptor polymer, independent of the type of polymer used with the interval $(T-T_g)$ likely to have significance. This supports the assumption that the large scale co-operative movement characteristic of T_g represents a large step-change in the diffusion coefficient of the solute molecule as a function of temperature. This coupling of diffusion to the glass transition may not be surprising given that the molecular weight of the dye is four to five times that of a typical repeating polymer unit. Additionally, the exclusive dependence of diffusivity on T_g implies that the diffusion coefficient of a particular solute at high temperatures, well above T_g, does not depend on the differences in interactions between the dye and the various dye-acceptor matrices. This may result from the high temperatures experienced by the dye and polymer matrices (150°C–300°C) by increasing free volume and reducing the effectiveness of intermolecular forces at high temperatures on diffusion coefficients. Recent work by Byers [46] on the diffusion of dyes in polycarbonate above T_g at 180°C agrees with this interpretation. Numerous dye structures were investigated, partly to explore the effects of intermolecular hydrogen bonding. It was found that dye diffusion in this constant matrix at this temperature was controlled by the shape of the dye molecule with no discernible effect of intermolecular forces on diffusion coefficients. However, at this time, it has not been proven that diffusion coefficients are unaffected by intermolecular forces in our systems. This assumption in our model may well be an oversimplification, and remains to be proven and hence, should certainly be treated as a first approximation.

Generally, for the materials used in this work, the solute component has the potential to self-associate whereas the polymer component does not. As described in the introduction, previous detailed infrared studies on the dye solute used in this work [37,38] have established the presence of both a dye–polymer intermolecular interaction between the dye hydroxyl group and the polymer electron-donating functional group (D–P) and a dye–dye self-association interaction between different dye hydroxyl groups (D–D). Eq. (4) was shown to be successful by considering only the dye–polymer specific interaction, with the dye–dye self-association interaction not being considered in the models developed. Further work to elucidate the effects of self-association will be reported in future when the transport of dye solutes with different numbers of hydroxyl groups will be reported [47].

4. Conclusions

The transport of a bihydroxyl azo dye solute was studied using dye diffusion thermal transfer printing. This dye was transferred from a constant dye-donor matrix to various dye-acceptor matrices well above the glass transition temperatures of the components. Under these conditions, dye transfer at a constant print time and for a constant temperature profile appears to be influenced by both kinetic and thermodynamic factors. Dye transport is adequately described as a function of diffusivity and solubility. The diffusivity is strongly influenced by the dye-acceptor polymer T_g. The solubility is controlled by the dye–polymer (acceptor) affinity resulting from the balance of endothermic physical forces and exothermic specific interactions. The former is described by solubility parameter differences between dye and dye-acceptor polymers while the latter is described by infrared frequency shifts of the dye O–H group resulting from specific intermolecular interaction between the dye hydroxyl group and the polymer electron-donating functional group.

Dye transfer was found to increase when the acceptor polymer T_g was lower and/or when the dye was more compatible with the dye-acceptor polymer. The latter is characterised by the combination of a closer solubility parameter match between the two components and a greater specific interaction between dye and dye-acceptor polymer. An excellent correlation was made for dye transport as a function of dye-acceptor polymer T_g, the solubility parameter difference between dye and dye-acceptor polymer and the dye hydroxyl infrared frequency shift. The hydroxyl vibrational frequency is an excellent measure of the specific interaction strength between dye and polymer when the electron-donating functional group is constant. When the polymer electron-donating functional group varies widely, the best model of the specific interaction strength is a quadratic function of the hydroxyl shift. This effect is caused by the different lengths of hydrogen bond formed with different types of polymer.

Acknowledgements

The authors would particularly like to thank Alan Butters (ICI Imagedata) for the numerous discussions which took place during the course of this work and to Peter Winter (ICI Imagedata) for his advice in the use of infrared spectroscopy. We would also like to acknowledge the synthetic skills of Roy Bradbury and Clive Mosscrop (Zeneca Specialties) for providing dye samples with controlled structures. Finally, we also wish to thank Robert Glen (ICI Imagedata) for allowing publication of this work.

References

[1] Stannett V. Diffusion in polymers. In: Crank J, Park GS, editors, London: Academic Press, 1968, Ch. 2.
[2] Kumins CA, Kwei TK. Diffusion in polymers. In: Crank J, Park GS, editors, London: Academic Press, 1968, Ch. 4.
[3] Fujita H. Diffusion in polymers. In: Crank J, Park GS, editors, London: Academic Press, 1968, Ch. 3.
[4] Barrer RM. J Phys Chem 1957;61:178.
[5] Meares P. J Am Chem Soc 1954;76:3415.
[6] Brandt WW. J Phys Chem 1959;63:1080.
[7] DiBeneditto AT. J Polym Sci 1963;A1:3459.
[8] Paul DR. Di Beneditto, AT. J Polym Sci 1964;A2:1001.
[9] Pace RJ, Datyner AJ. J Polym Sci, Polym Phys Ed. 1979;17: 437, 453, 465, 1675.
[10] Pace RJ, Datyner AJ. J Polym Sci Polym Phys Ed 1980;18:1103.
[11] Bueche F. J Chem. Phys. 1953;21:1850.
[12] Ferry JD. Viscoelastic properties of polymers, 2nd ed. New York: Wiley, 1970.
[13] Fujita H, Kishimoto A, Matsumoto K. Trans Faraday Soc 1960;56:424.
[14] Cohen MH, Tumbull D. J Phys 1959;31:1164.
[15] Vrentas JS, Duda JL. J Poly Sci Polym, Phys Ed 1977;15:403.
[16] Vrentas JS, Duda JL. Macromolecules 1976;9:785.
[17] Maurtiz KA, Storey RF, George SE. Macromolecules 1990;23:441.
[18] Maurtiz KA, Storey RF. Macromolecules 1990;23:2033.
[19] Sweet GE, Bell JP. Text Res J 1976;46(6):447.
[20] Chantrey G, Rattee ID. J Appl Pol Sci 1974;18:93.
[21] McGregor R, Peters RH. Ramachandran. C.R. 1968; J Soc Dyers Colour 84:9.
[22] Hossain TMA, Maeda H, Iijima T, Morita Z. J Poly Sci Lett 1967;5:1069.
[23] Shibusawa T. J Poly Sci Part B: Poly Phys 1993;31:29.
[24] Williams ML, Landel RF, Ferry JD. J Am Chem Soc 1955;77:3701.
[25] Zhang J, Wang BH. Macromolecules 1987;20:683.
[26] Zhang J, Wang BH. Macromolecules 1987;20:2296.
[27] Ehlich D, Siliescu H. Macromolecules 1990;23:1600.
[28] Slark AT. European Polymer Journal 1997;33(8):1369.
[29] Hann RA, Beck NCJ. Imaging Technology 1990;16:238.
[30] Hann RA, unpublished results.
[31] Shinozaki K, Hirano H. Journal of Imaging Science and Technology 1994;38(6):571.
[32] Slark AT. Polymer 1997;38(10):2407.
[33] Slark AT. Polymer 1997;38(17):4477.
[34] Slark AT. Polymer 1998; in press.
[35] Shearmur TE, Drew DW, Clough AS, van der Grinten MGD, Slark AT. Polymer 1996;37(13):2695.
[36] Slark AT, Fox JE. Polymer 1997;38(12):2989.
[37] Slark AT, Hadgett PM. Polymer 1998;39(10):2055.
[38] Slark, AT, Hadgett, PM. Polymer 1998; in press.
[39] Slark AT, Hadgett PM. Polymer 1998;39(17):3977.
[40] Fedors RF. Polym Eng Sci 1974;14:147.
[41] van Krevelen DW. Properties of Polymers, Elsevier Science, 1986.
[42] dev Naylor T. Comprehensive polymer science. In: Allen G, Bevington JC, editors. Oxford: Pergamon Press, 1989, Ch. 20, Vol. 2.
[43] Coleman MM, Graf JF, Painter PC. Specific interactions and the miscibility of polymer blends, Technomic Publishing Company, 1991.
[44] Murthy ASN, Rao CNR. Appl Spect Rev 1968;2(1):69.
[45] Pimentel GC, McCellan AL. Ann Rev Phys Chem 1971;22:3247.
[46] Byers GW. Macromolecules 1993;26:4242.
[47] Slark AT, Hadgett PM. Polymer 1998; to be published.